*Int. J. Mol. Sci.* **2003**, *4*, 572-585

International Journal of
**Molecular Sciences**
**ISSN 1422-0067**

www.mdpi.org/ijms/

# Cationic Polymerization of 1,2-Epoxypropane by an Acid Exchanged Montmorillonite Clay in the Presence of Ethylene Glycol

**Ahmed Yahiaoui, Mohammed Belbachir*, and Aïcha Hachemaoui**

Laboratoire de chimie des polymères, Département de Chimie, Faculté des Sciences, Université d'Oran, BP 1524 El'Menouer Oran 31000 Algérie. Fax:213 41 51 00 57, E-mail: yahmeddz@yahoo.fr

*Received: 7 May 2003 / Accepted: 14 October 2003 / Published: 27 October 2003*

**Abstract:** The polymerization of propylene oxide (PO) catalysed by maghnite-$H^+$ (mag-$H^+$) in the presence of ethylene glycol was investigated. Mag-$H^+$ is a montmorillonite silicate sheet clay was prepared through a straight forward proton exchange process. It was found that the cationic polymerization of PO was initiated by mag-$H^+$ at 20 °C both in bulk and in solution. The effect of the amount of mag-$H^+$ and solvent was studied. These results indicated the cationic nature of the polymerization A possible initiation pathway, *via* the transfer of protons from mag-$H^+$ to the monomer, is proposed.

**Keywords:** maghnite, montmorillonite, catalyst, epoxides, propylene oxide, ring opening polymerization.

## Introduction

Montmorillonite is a naturally occurring clay which has the ideal formula $Al_2O_3.SiO_2.HOH+nH_2O$. When pre-treated with strong acids, the mineral may be used, for example, as a bleaching clay or in reactions which would otherwise be catalysed using proton or Lewis acids, such as the polymerizations of tetrahydrofuran [1] and epoxides [2]. Recently, monomers were found to intercalate into lattice layers of montmorillonite clay, permitting *in situ* polymerizations yielding polymer/clay nano-composites. Several polymers, for example, polyamide (nylon-6) [3], polystyrene (PS) [4-8], and polystyrene-*block*-polyisoprene-*block*-polystyrene[9], have been prepared *via* this route.

The cationic polymerization of epoxides, in the presence of hydroxyl-containing compounds, proceeds *via* two competitive mechanisms [10-18]:

(i) the *active chain end mechanism* (ACEM) in which three membered cyclic tertiary oxonium ions constitute the growing species, as detailed in Scheme 1 (a). Propagation is accompanied in this case by end-biting and back-biting reactions, giving rise to cyclics (di-, tri- or tetramer, depending on the epoxide used); and

(ii) the *activated monomer mechanism* (AMM) in which propagation involves the addition of an activated (e.g., protonated) monomer onto the hydroxyl end-group of the initiator or the growing macromolecule, as shown in Scheme 1 (b).

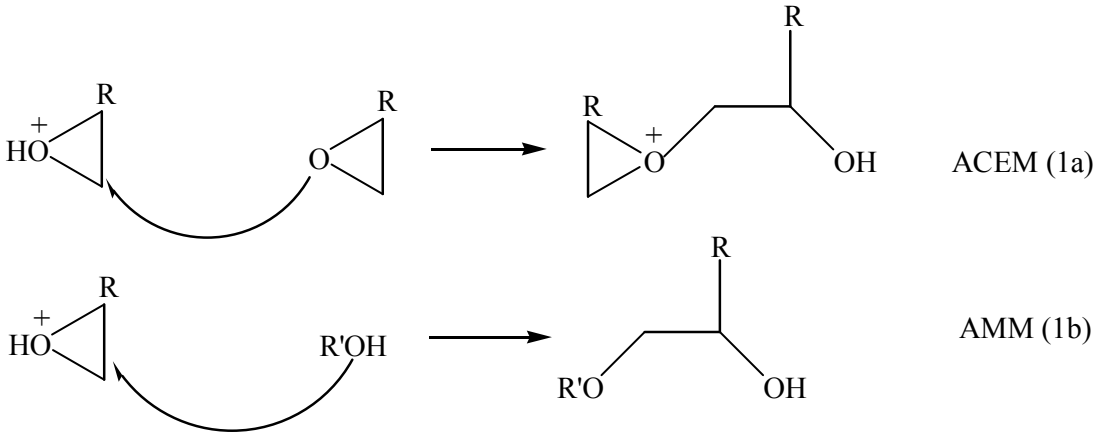


(R'OH: initiator or growing macromolecules)

**Scheme 1**

In order to limit the formation of cyclic oligomers in these reactions and therefore reduce the possibility of the reaction following the pathway shown in Scheme 1(a), it is necessary to add the monomer slowly to the reaction medium so as to increase the probability that the monomer will be protonated and then go on to react with the present nucleophiles. If, as here, the chain end of the epoxide polymer is an alcohol, the addition of the protonated monomer effectively leads to the reformation of the alcohol chain end. If this is the dominant process, the formation of cyclic oligomers may be suppressed. It is worth noting that using a diol as initiator and $HBF_4$ as catalyst, Penczek prepared telechelic oligomers of epichlorohydrin and propylene oxide (PO) [19,20].

The cationic polymerization of alternative epoxides in the presence of diols have also been studied. For example, Xu *et al.* [21] studied the case of 1,2-epoxy-3-nitropropane (ENP) with 1,3-butane-diol as initiator. The authors indicated the formation of oligomers with $M_n$ = 1100 g $mol^{-1}$, however, the end groups of these systems were not presented. Poly(propylene oxide) (PPO), another 1,2-epoxide, is widely used in industrial applications. For example, PPO diols and higher polyols are used for the preparation of polyurethanes and polyurethane elastomers. However, the cationic initiators used to make PPO are expensive and often give rise to impurities, such as chromium, mercury or antimony, in the end product which often render the material unsuitable for medical or veterinary applications and make its disposal in the environment problematic. In addition, such initiators require the use of very

high or very low temperatures and high pressures during the polymerization reaction, and lead to relatively poor yields.

The purpose of this paper is to study the cationic polymerisation of PO using a montmorillonite clay which has undergone a proton exchange process (mag-$H^+$), a new, non-toxic cationic catalyst for heterocyclic monomers [22]. In contrast to the more usually used catalysts, mag-$H^+$ can be easily separated from the polymer and regenerated by heating to a temperature above 100 °C[23,24]. The effects of the relative amounts of mag-$H^+$ and solvent used, and eventually, the mechanism, are discussed.

## Experimental

*Materials*

1,2-Propylene oxide (PO) and ethylene glycol (EG) were purified by fractional distillation. Dichloromethane and toluene were purified following standard techniques and used after distilling over their respective drying agents. These chemical were obtained from Aldrich.

Montmorillonite clay, or 'raw-maghnite' was obtained from ENOF Maghnia (Western of Algeria). The protonated forms of montmorillonite (mag-$H^+$) were prepared by shaking the clay in a solution of sulfuric acid until saturation was achieved (normally after 2 d at room temperature). The cation-exchanged clay was then recovered by filtration, and again suspended in deionized water. This process was repeated until no sulfate ions were indicated present in the filtrate using $BaCl_2$. The mag-$H^+$ was then isolated by filtration, dried at 105 °C and then finely ground. The cation exchange capacity (CEC) of the clay was found to be 84 mEq $(100\ g)^{-1}$ of dried clay. Sulfuric acid of concentrations 0.05 M, 0.10 M, 0.15 M, 0.20 M, 0.25 M, 0.30 M and 0.35 M were used to prepare the samples, respectively, denoted mag-$H^+$ 0.05 M, mag-$H^+$ 0.10 M, mag-$H^+$ 0.15 M, mag-$H^+$ 0.20 M, mag-$H^+$ 0.25 M, mag-$H^+$ 0.30M and mag-$H^+$ 0.35 M.

Polymerizations were performed with or without dichloromethane at 20 °C. The procedure was identical in both cases, involving slow addition of PO to the stirred bulk EG containing catalyst or the solution in dichloromethane. Prior to use, mag-$H^+$ was dried at 120 °C overnight and then transferred to a vacuum desiccator containing $P_2O_5$ to cool to room temperature overnight. An example reaction is detailed here. After charging the reaction vessel with the mineral (0.1g) and EG (0.086 mol), PO (10 g, 0.172 mol) was slowly added. At the required time, an aliquot of the reaction mixture was then taken in such manner as to exclude any clay mineral. At the end of the reaction, the resulting mixture was dissolved in dichloromethane, filtered to remove the clay and then dried under vacuum to yield the polymer (yield of this example was 77 %).

*Characterization*

Viscosity-average molecular weights ($M_v$s) and intrinsic viscosity ($\eta$) measurements were performed at 35 °C in toluene using a Sematech® (Viscologic TL1) capillary viscometer. Gel permeation chromatography (GPC) was performed using a Waters® model 200 instrument equipped with 4 styragel columns in series ($10^3$ Å, $10^4$ Å, 1.5 x $10^5$ Å and 3 x $10^6$ Å). Tetrahydrofuran was used as eluent at a flow rate of 1 mL $min^{-1}$, and characterizations were performed against a series of 9 poly(ethylene oxide) standards. Hydroxyl groups were determined by reacting the solution of polymer in $CDCl_3$ with a 2 fold excess of $(CF_3CO)_2O$, followed by determination of $CF_3COO\underline{CH_2}$-(4.20 ppm δ) and $CF_3COO\underline{CH}$-(5.17 ppm δ) groups. Thermal gravimetric (TGA) characterisations were performed under nitrogen using a Dupont model 9900 thermal analyser at a heating rate of 20 °C $min^{-1}$.

Maghnite and mag-$H^+$ samples were characterised by XRF (a Philips PW 2400XRF spectrometer at the Laboratory of Inorganic Chemistry, Granada University, Spain) using the $LiB_4O_7$ fusion method. XRD profiles for pressed powder samples were recorded on a Philips PW 1710 diffractometer using Cu-K α radiation (λ =1.5418 Å). IR absorption spectra were recorded on a ATI Matson FTIR N°9501165 spectrometer using the KBr pressed discs which were made up of 0.5 mg of sample in 300 mg KBr. High-resolution solid-state $^{29}Si$ and $^{27}Al$ MAS NMR spectra of untreated (raw-maghnite) and acid treated (mag-$H^+$ 0.25 M) samples were recorded on a Brüker ASX 500 spectrometer at 59.6 and 130.3 MHz, respectively. The sample spinning frequency was 4 KHz for $^{29}Si$ and 11.5 KHz for $^{27}Al$.

## Results and Discussion

*Catalyst Structure*

Various methods of analysis, such as $^{27}Al$ and $^{29}Si$ MAS NMR, show that Maghnite is a montmorillonite sheet silicate clay. The elementary analysis of the selected samples obtained using XRF is as settled in the following Table 1. It is necessary to report that the best value of PO conversion obtained with mag-$H^+$ 0.25 M, for this reason we kept this sample to study the effect of catalyst proportions and solvent on PO polymerization. Acid treatment of raw-maghnite was indicated to cause a relative reduction in the content of octahedrally spaced $Al_2O_3$ and a relative increase in silica ($SiO_2$).

Table 2 shows the various types of montmorillonites studied, and can see that Maghnite has 11.9 % more $SiO_2$ than that from Wyoming 19.35 than from Montmorillon (Vienne, French). When treated with sulfuric acid, this difference is even greater; 14.21 % and 21.66 % as compared to Wyoming and Vienne Bentonite, respectively. Maghnite contains 5.60 % and 5.49 % less $Al_2O_3$, than the Wyoming and Vienne Bentonites, respectively.

Figures 1(a) and 1(b) and Table 3 show X-ray diffraction patterns of raw-maghnite and Mag-$H^+$. The basal spacing of the raw-Maghnite was exhibited 15.02 Å. The titration of raw-maghnite with 0.25 $H_2SO_4$ resulted in the exchange of exchangeable cations for $H^+$ in the interlayer. The X-ray powder diffraction of the dried Mag-$H^+$, as shown in Figure 1(b), exhibited 00 *l* reflections corresponding to

**Table1.** Elementary compositions of Protons exchanged samples "Maghnite" compositions wt%.

| | Composition wt% | | | | | | | | | | |
|---|---|---|---|---|---|---|---|---|---|---|---|
| Sample | $SiO_2$ | $Al_2O_3$ | $Fe_2O_3$ | CaO | MgO | $Na_2O$ | $K_2O$ | $TiO_2$ | $SO_3$ | As | PF* |
| Raw-Maghnite | 69.39 | 14.67 | 1.16 | 0.30 | 1.07 | 0.50 | 0.79 | 0.16 | 0.91 | 0.05 | 11 |
| H-Mag0.05M | 70.75 | 14.67 | 1.05 | 0.30 | 1.01 | 0.49 | 0.78 | 0.16 | 0.75 | 0.04 | 10 |
| H-Mag0.10M | 71.00 | 14.60 | 1.00 | 0.30 | 0.98 | 0.39 | 0.78 | 0.16 | 0.55 | 0.04 | 10 |
| H-Mag0.15M | 71.58 | 14.45 | 0.95 | 0.29 | 0.91 | 0.35 | 0.77 | 0.15 | 0.42 | 0.03 | 10 |
| H-Mag0.20M | 71.65 | 14.20 | 0.80 | 0.28 | 0.85 | 0.30 | 0.77 | 0.15 | 0.39 | 0.01 | 10 |
| H-Mag0.25M | 71.70 | 14.03 | 0.71 | 0.28 | 0.80 | 0.21 | 0.77 | 0.15 | 0.34 | 0.01 | 11 |
| H-Mag0.30M | 73.20 | 13.85 | 0.70 | 0.27 | 0.78 | 0.20 | 0.76 | 0.13 | 0.31 | 0.02 | 9.78 |
| H-Mag0.35M | 75.31 | 13.52 | 0.71 | 0.26 | 0.78 | 0.18 | 0.75 | 0.13 | 0.32 | 0.01 | 8.03 |

*PF: Pert in Fire

**Table 2.** Comparison in the composition (in %) of American, French and Maghnia Algerian Bentonites.

| | Wyoming (USA)[25] | Vienne (France)[26] | Raw-Maghnite (Algeria) | H-Maghnite (Algeria) |
|---|---|---|---|---|
| $SiO_2$ | 50.04 | 57.49 | 69.39 | 71.70 |
| $Al_2O_3$ | 20.16 | 20.27 | 14.67 | 14.03 |
| $Fe_2O_3$ | 0.68 | 2.92 | 1.16 | 0.71 |
| FeO | | 0.19 | | |
| CaO | 1.46 | 0.23 | 0.30 | 0.28 |
| MgO | 0.23 | 3.13 | 1.07 | 0.80 |
| $K_2O$ | 1.27 | 0.28 | 0.79 | 0.77 |
| $Na_2O$ | Tr | 1.32 | 0.5 | 0.21 |
| $TiO_2$ | | 0.12 | 0.16 | 0.15 |
| $SO_3$ | | | 0.91 | 0.34 |
| As | | | 0.05 | 0.01 |

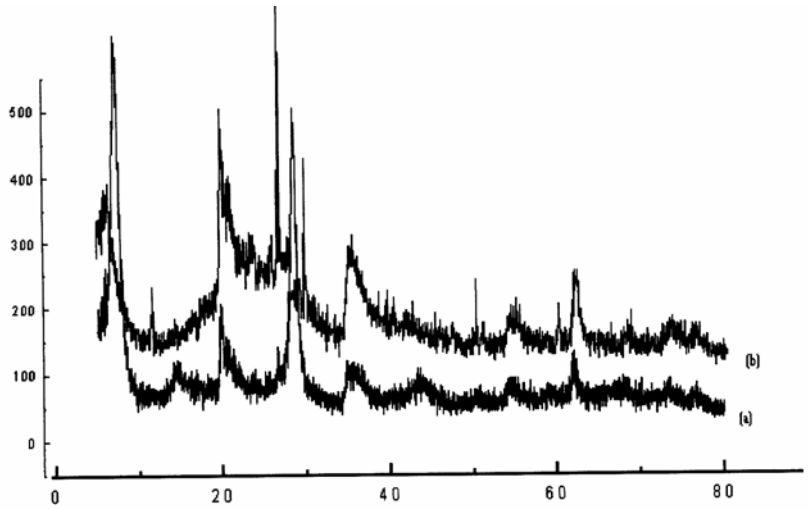


**Figure 1.** X-ray Power Diffraction of (a) "Raw-Maghnite" and (b) "Mag-$H^+$0.25M"

**Table 3:** RX characteristic of Raw-Maghnite and Mag-$H^+$0.25M.

| Samples | $d_{hkl}$ (A°) | hkl | Nature of sample |
|---|---|---|---|
| Raw-Maghnite | 12.50 | 001 | Montmorillonite |
| | 4.47 | 110 | Montmorillonite |
| | 4.16 | ,, | Quartz |
| | 3.35 | ,, | Quartz |
| | 3.21 | ,, | Feldspath |
| | 3.03 | ,, | Calcite |
| | 2.55 | 200 | Montmorillonite |
| | 1.68 | 009 | Montmorillonite |
| | 1.49 | 060 | Montmorillonite |
| Mag-$H^+$0.25M | 15.02 | 001 | Montmorillonite |
| | 4.47 | 110 | Montmorillonite |
| | 4.16 | ,, | Quartz |
| | 3.35 | ,, | Quartz |
| | 3.21 | ,, | Feldspath |
| | 3.03 | ,, | Calcite |
| | 2.55 | 200 | Montmorillonite |
| | 1.68 | 009 | Montmorillonite |
| | 1.49 | 060 | Montmorillonite |

basal spacing of 12.5 Å. Yun Kwon *et al*[27] reported that the decrease in the basal spacing indicates a loss of the interlayer $H_2O$ upon the replacement of $Na^+$ for $H^+$. In particular, although the X-ray peak of the montmorillonite did not change substantially before or after the acid treatment, there was a decrease in the basal spacing. This implies that the original structure was well preserves after the acid treatment.

The effects of the acid activation process on the FTIR spectrum of the treated Maghnite (Fig. 2) are summarised as follows: The intensity of the absorption band at 3630 $cm^{-1}$ (AlAlOH coupled by AlMgOH stretching vibrations) decreases with acid treatment. The bands at 3425 $cm^{-1}$ and 3200 $cm^{-1}$ (absorption of interlayer water) become more diffuse with acid treatment [28]. The intensity of the Si-O out of plane and Si-O-Si (2 bands) in plane stretching bands at 1116, 1043 and 999 $cm^{-1}$ have not been affected by acid treatment. The AlAlOH (920 $cm^{-1}$), $AlFe^{3+}OH$ (883 $cm^{-1}$) and AlMgOH (846 $cm^{-1}$) deformation bands decrease with acid treatment. The intensity of the band at 796 $cm^{-1}$ increases with treatment, reflects alterations in the amount of amorphous silica in accordance to the findings of others workers [29,30]. The intensity of the band at 628 $cm^{-1}$ (either Al-OH or Si-O bending and / or Al-O stretching vibration) gradually decreases with acid treatment in good agreement with the findings of Komadel [31]. The intensity of the band at 467 cm-1 (Si-O-Al and Si-O-Mg coupled by OH vibration or Si-O bending vibrations) is essentially unchanged.

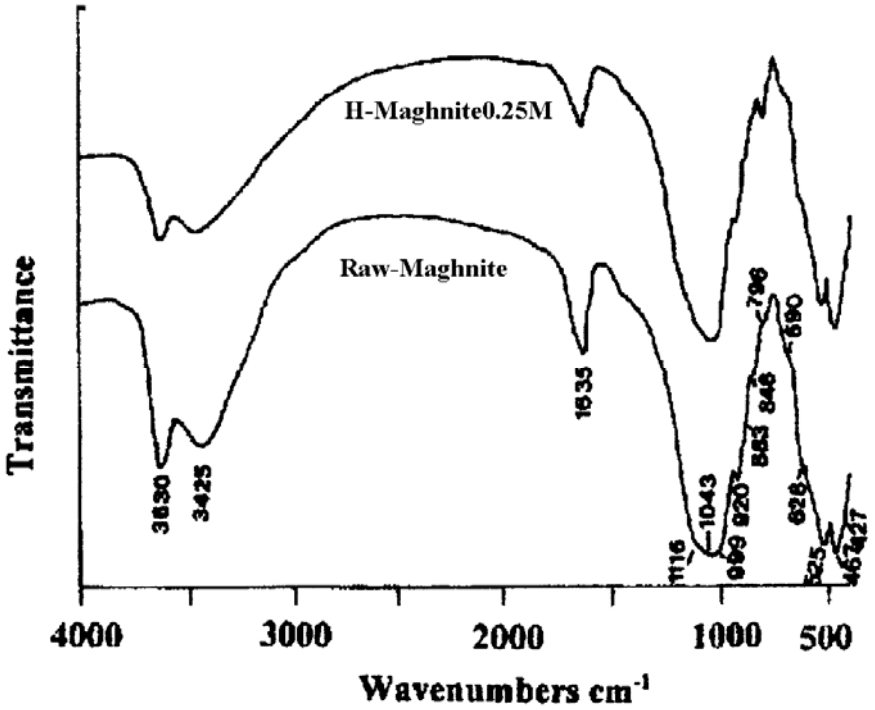


**Figure 2.** IR Spectra of (a) untreated Clay "Raw-Maghnite" and (b) Acid treated Clay "Mag-$H^+$0.25M"

$^{27}$Al NMR spectra of both raw-maghnite and mag-$H^+$ 0.25 M are given in Fig 3. The spectra of Maghnite exhibits mainly the typical resonance at 2.9 ppm of octahedral aluminium ($^{[6]}$Al) in a phyllosilicate but also a small but significant contributions at 60 and 68 ppm assigned to aluminium tetrahedrally co-ordinated to oxygen ($^{[4]}$Al) [32,33].

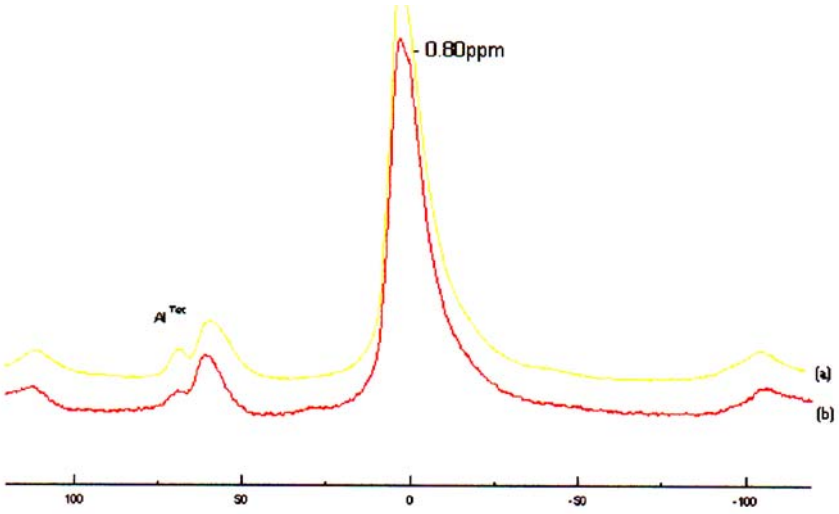


**Figure 3.** $^{27}$Al MAS NMR spectra of (a) "Raw-Maghnite" and (b) "Mag-$H^+$0.25M"

The $^{29}$Si MAS NMR spectra for the raw-maghnite and Mag-$H^+$ 0.25M are shown in Fig 4. The dominant resonance at – 93.5 ppm corresponds to Q 3 (OAl) units, *i.e.* $SiO_4$ groups cross linked in the tetrahedral sheets with no aluminium in the neighbouring tetrahedral [34]**.** The resonance at –112 ppm corresponds to three-dimensional (3D) silica with no aluminium present, designed Q 4 (OAl) [27,34].

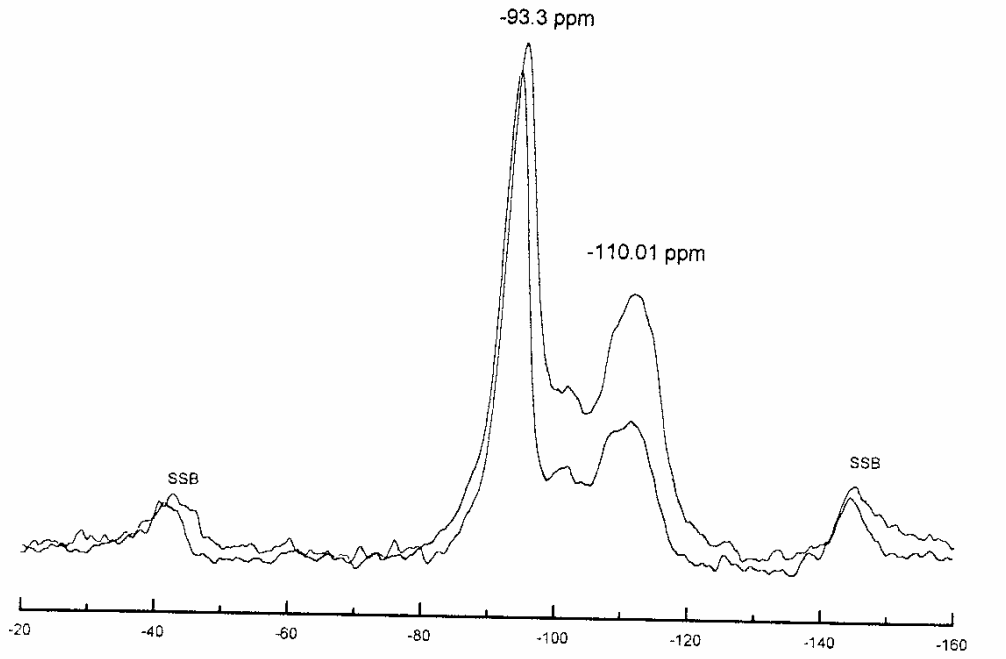


**Figure 4.** $^{29}$Si MAS NMR spectra of (a) "Raw-Maghnite" and (b) "Mag-$H^+$0.25M"

*Polymerization and Products Characterization*

The results of experiments of PO polymerization induced by Mag-$H^+$ 0.25M are reported in Table 4. For all these experiments the temperature was kept constant at 20 °C for 2 h.

**Table 4.** Polymerization of PO induced by the "Mag-$H^+$0.25M"

| Experiment | PO (g) | [PO] | "H-Maghnite0.25M"(g) | Yield % | Mv | $M_n$ | $M_w$ | $I=M_w/M_n$ |
|---|---|---|---|---|---|---|---|---|
| 1 (Bulk) | 10 | - | 0.1 | 15 | 520 | 349 | 771 | 2.21 |
| 2 (Bulk) | 10 | - | 0.05 | 04 | 910 | 746 | 993 | 1.33 |
| 3 ($CH_2Cl_2$) | 5 | 5 | 0.1 | 11 | 896 | 610 | 1050 | 1.72 |

*Effect of Mag-$H^+$ 0.25M Proportion*

Table 5 and Figure 5 show the effect of the amount of Mag-$H^+$ on the polymerization rate of PO. As can be noted in this figure, the polymerization rate increased with the amount of Mag-$H^+$. These results clearly indicate that an optimal rate of reaction is obtained at room temperature by polymerizing PO in bulk with Mag-$H^+$ proportion equal to 1 %. Under these conditions, monomer conversion reaches 80 %

**Table 5.** PO conversions with time: for 10g of PO, the amounts of Mag-$H^+$0.25M were: a)0.1g, b)0.05g

| Time(h) | 2 | 6 | 9 | 15 | 18 | 20 | 22 | 26 | 30 |
|---|---|---|---|---|---|---|---|---|---|
| Yield(%)(a) | 15 | 21 | 30 | 42 | 52 | 60 | 67 | 77 | 80 |
| Yield(%)(b) | 4 | 15 | 26 | 30 | 35 | 39 | 50 | 52 | 54 |

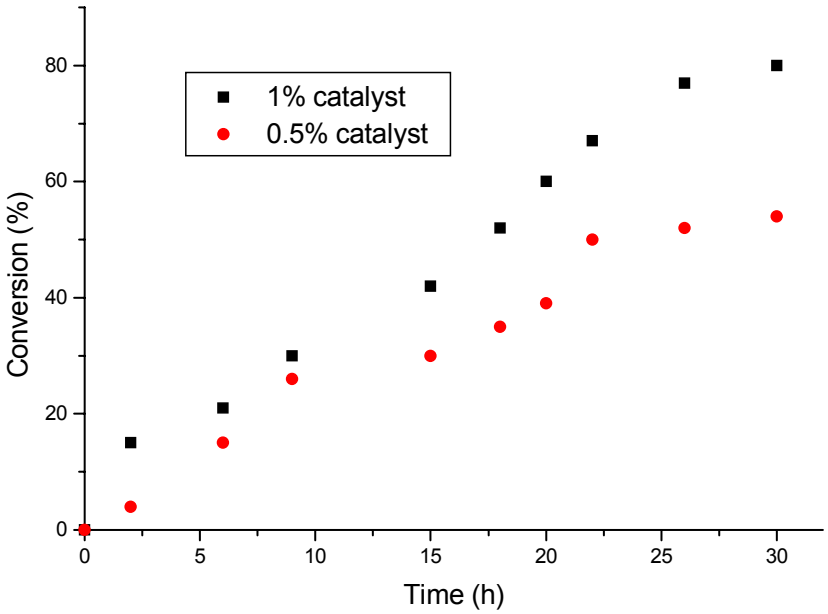


**Figure 5.** Effect of catalyst proportion upon the conversion of Propylene oxide.

after 30 h. Similar results are obtained by Belbachir *et al*[23,24], and Njopwouo *et al*[35], in the polymerization of *N*-vinyl pyrrolidone and THF by Mag-$H^+$ and the polymerization of styrene by montmorillonite, respectively.

In contrast, as depicted in Figure 6, the molecular weight is inversely proportional to the amount of Mag-H. This finding is in good agreement with the proposal that Mag-H is present as the active initiator species since the number of those species should be related to their surface area. Similar results are obtained by Kadakowa *et al.* [36], and Crivello *et al*. [37], in the polymerization of lactones by Sn-montmorillonite and cyclohexene oxide by Cobalt respectively.

*[1] H-NMR Study*

An investigation was devoted to the analysis of the PPO by $^1$H NMR spectroscopy at 200 MHz (Table 6 and Fig. 7).

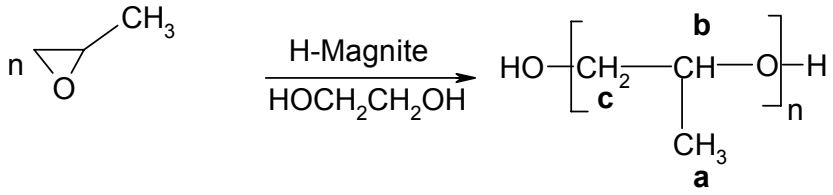


**Scheme 2**

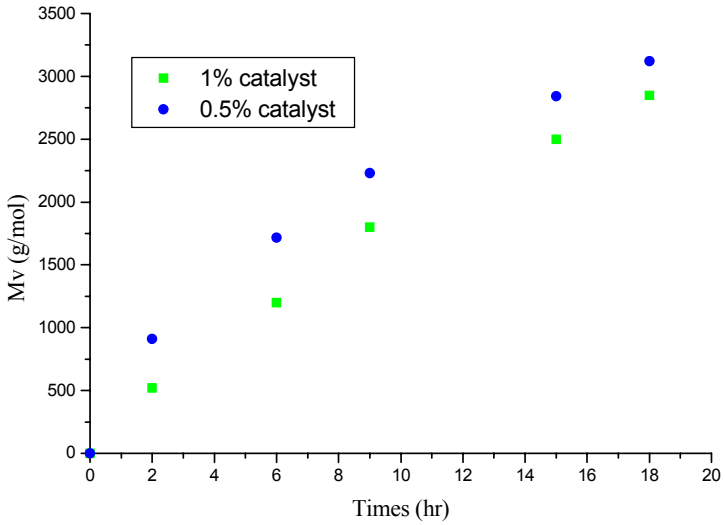


**Figure 6.** Effect of catalyst proportion upon the viscosimertic molecular weight.

**Table 6.** Chemical shift of polymers protons

| Proton type | (a) | (b) | (c) |
|---|---|---|---|
| δ(ppm) | 1.1 | 3.5 | 3.5 |

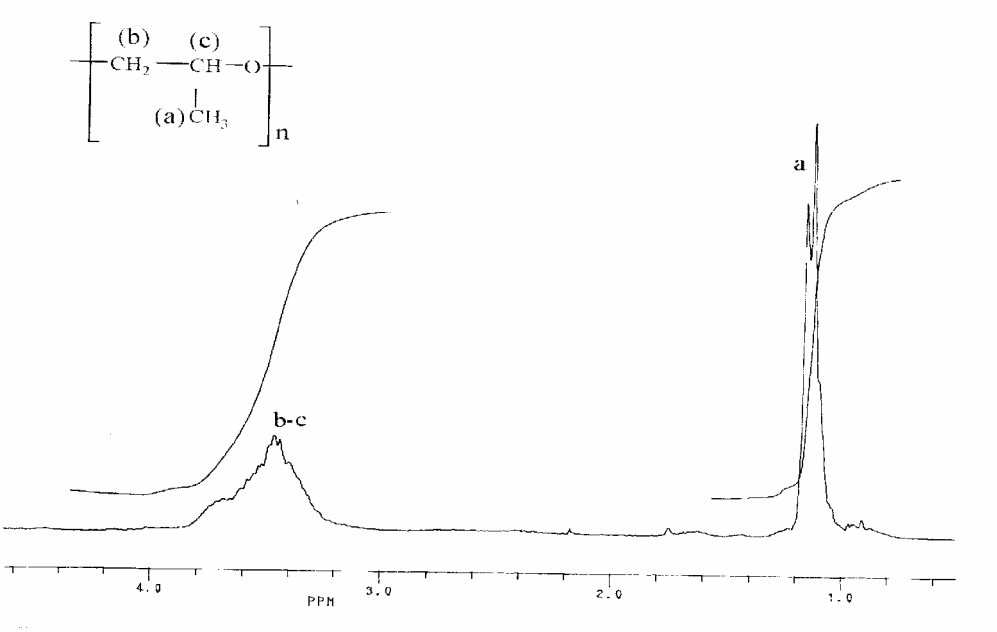


**Figure 7.** 200 MHz $^{1}$H-NMR spectrum of PPO in $CDCl_3$.

According to the work published by Oguni *et al*[38] and Ishimori *et al*[39] $^1$H NMR spectroscopy at 200 MHz (Solvent CDCl3) (Fig. 7) consist of a broad doublet centred at ca 1.1 ppm ($CH_3$) and complex multiplet centred at ca. 3.5 ppm ($C\underline{H}_2$-O , C$\underline{H}$-O).

*End-Groups*

$^1$H-NMR method was used for the end-groups analysis. Two types of end-groups, primary and secondary hydroxyl groups may be present in PPO diols.

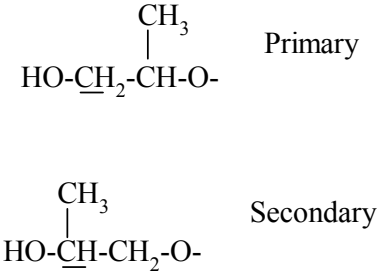


(2)

The signals of protons in the groups underlined in reaction (2) are to close to the corresponding signals from the chain, therefore hydroxyl end-groups were converted into the ester groups by reaction with trifluoroacetic anhydride. Thus, fourfold excess of $(CF_3CO)_2O$ was added directly to the NMR tubes containing solution of PPO diol. The spectrum is shown in Fig. 8 together with the relevant assignment. A small doublet at 1.27 ppm related to the methyl groups at the esterified hydroxyl groups $CF_3COOCH(\underline{CH}_3)CH_2$- and $CF_3COOCH_2CH(\underline{CH}_3)$-. The distorted doublet at 4.20 ppm is due to the protons in methylene group $CF_3COO\underline{CH}_2CH(CH_3)$- and the sextet at 5.17 ppm is due to the proton in the methine group $CF_3COO\underline{CH}(CH_3)CH_2$-

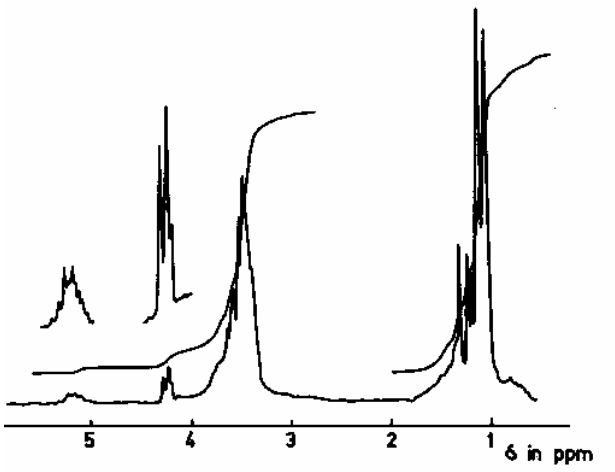


**Figure 8.** 200 MHz $^1$H-NMR spectrum of poly(propylene oxide) after esterification with $(CF_3CO)_2O$ in $CDCl_3$.

The large amount of secondary hydroxyls shows that, for steric reasons, the activated monomer is preferentially attacked on the carbon atom located in the β position with regard to the $CH_3$ group, as it is illustrated below:

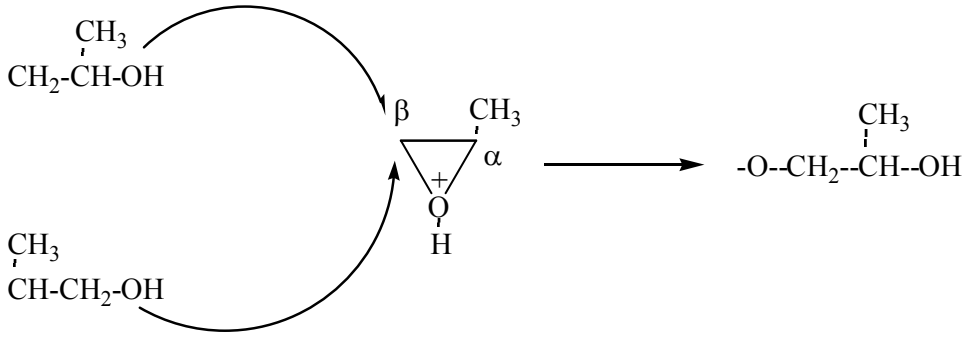


Similar results were obtained by Penczek and Lagarde in the case of epichlorhydrin and 1,2-epoxy-3-nitropropane [16,17].

*Effect of Solvent*

The data in Table 3 indicates that polymerizations carried out in solution leaded to higher molecular weights and narrower molecular weight distributions (MWDs) ($M_w/M_n$). However, conversions in solution were smaller than the ones obtained in bulk polymerisation. Low conversions in solution polymerization may be explained by the difficult contact in heterogeneous phase, between monomer particles and the "initiating active sites" of "catalyst" surface.

*Polymerization Mechanism*

PO may be polymerized *via* a cationic pathway. According to the preceding discussion and the results of product analysis, we propose a cationic mechanism for the resulting reaction of polymerization initiated by Mag-$H^+$ 0.25 M. Protons carried by montmorillonite sheets of Mag-$H^+$ 0.25 M initiated the cationic polymerization, these montmorillonite sheets take place as counter-anions. Propagation then takes place by conventional cationic mechanism.

*Initiation*

Protons carried by montmorillonite sheets of Mag-$H^+$ 0.25 M induced the polymerization; these montmorillonite sheets take place as counter-anions.

The first stage is the protonation of PO. The formed ions oxonium take place in the vicinity of the counter-anion carried by montmorillonite sheets, as in:

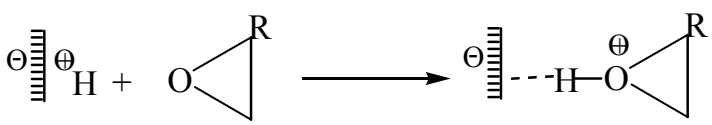

*Propagation*

Then a molecule of EG attacks in a nucleophilic way protonated PO.

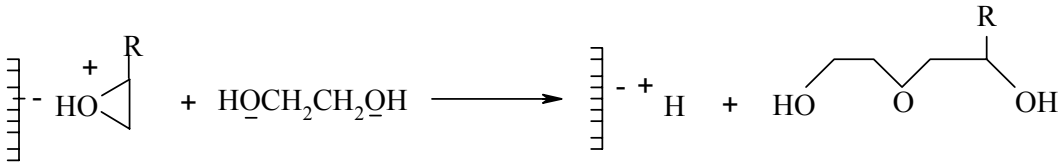

Subsequently, there is a nucleophilic attack of the oxygen of hydroxyl of the chains in growth on the carbon atom located in the β position with regard to the $CH_3$ group

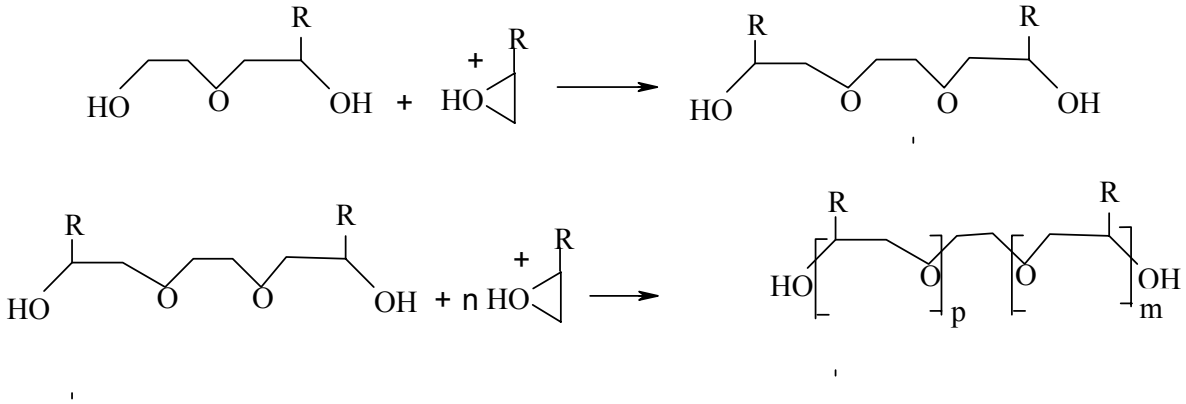

## Conclusion

In conclusion, we have found that acid-exchanged maghnite is effective as acidic catalyst for the ring opening polymerization of PO. The polymerization catalysed by Mag-$H^+$, in the presence of ethylene glycol proceeds by activated monomer mechanism (AMM) to yield PPO. The polymerization proceeds smoothly, and a simple filtration is sufficient to recover the catalyst.

## Acknowledgements

The authors wish to thank Dr. Roger Hiorns, University of Pau and Ador Region, for his support and encouragement.

## References

1. Mueller, H.; Huchler, O. H and Hoffmann, H. *US Patent.* **1981**, 4 243 799.
2. Farbenfabriken Bayer, *German Patent.* **1959**, 1 049 103.
3. Fujita, K.; Ishida, Y and J.Suezana, Japan Kokai Tokkyo Toho, JP, **1987**, 62 289 537.
4. Vu Moc, T.; Petit, H and Maitte, P. *Bull. Soc. Belg,* **1982**, *91*, 261.
5. Schelly, J. S.; Mather, P. T and DeVries, K. L. *Polymer*. **2001**, *42*, 5849.
6. Vaia, R. A.; Jandt, K. D.; Kramer, E. J and Giannelis, E. P. *Macromolecules*. **1995**, *28*, 8080.

7. Vaia, R. A and Giannelis, E. P. *Macromolecules*. **1997**, *30*, 7990.
8. Yoon, J. T.; Jo, W. H.; Lee, M. S and Ko, M. B. *Polymer*. **2001**, *42*, 329.
9. Lee, J.; Park, M. S.; Yang, H. C.; Cho, K and Kim, J. K. *Polymer*. **2003**, *44*, 1705.
10. Dreyfuss, M. P. *J. Macromol. Sci. Chem*. **1975**, *A9*, 729.
11. Kern, R. J. *J.Org. Chem*. **1968**, *33*, 388.
12. Libszowski, J.; Szymanski, R and Penczek, S. *Makromol.Chem*. **1989**, *190*, 1225.
13. Biedron, T.; Kubisa, P and Penczek , S. *J. Polym. Sci.: Pt A*: *Polym Chem*. **1991**, *29*, 619.
14. Tokar, R.; Kubisa , P.; Penczek, S and Dworak A. *Macromolecules.* **1994**, *27*, 320.
15. Bednarek , M.; Kubisa, P and Penczek, S. *Makromol.Chem.Suppl* . **1989**, *15*, 49.
16. Biedron, T.; Szymanski, R.; Kubisa, P.; Penczek, S. *Makromol. Chem, Macromol. Symp*. **1990**, *32*, 155.
17. Lagarde, F.; Reibel, L and Franta, E. *Makromol.Chem*. **1992**, *193*,1087.
18. Weiss, A. *Angew. Chem. Int*, *Ed.* **1981**, *20*, 850.
19. Wojtania, M.; Kubisa, P and Penczek, S. *Makromol. Chem. Symp*. **1986**, *6*, 201.
20. Kubisa, P. *Makromol. Chem. Symp*. 1988, 13/14, 203.
21. Xu, Y.; Dong, S.; Fan, C.; Wang, W.; Den, K and Zhow, M. Z. *Gaoefenzi Tongxun*. **1981**, *5*, 368.
22. Belbachir, M and A. Bensaoula, *US Patent*. **2001**, 6 274 527 B1.
23. Meghabar, R.; Megherbi, A and Belbachir, M. *Polymer* (*in press*).
24. Ferrahi, M.I and Belbachir, M. *Int. J. Mol. Sci*. **2003**, *4*, 312.
25. Montmorillonite. Montmorillon (Vienne,France), Damour, *An. Ph. Ch*. **1847**, *21*, 376.
26. Bentonite, Upton, Wyoming (USA), Analytical Data Reference, *Clay Min*, Report N° 7. *Amer. Petro*. Int. Project 49, **1950**.
27. Yun Kwon, O.; Won Park, K and Young Jeong, S. *Bull. Korean Chem. Soc.* **2001**, *22(7)*, 679.
28. Farmer, V. C. In *Infrared Spectra of Mineral*s, Farmer, V. C., Ed, *Mineralogical Society*, London. **1974**, 331.
29. Moeke, H. H. W. In *Infrared Spectra of Mineral*s, Farmer, V. C., Ed.; Mineralogical Society: London. **1974**, 365.
30. Madejovà, J.; Bednànikovà, E.; Komadel, P and Cicel, B. *in Proc.11 th Conf. Chem. Miner. Petrol.Ceske Budéjovica* 1990; Konta, J., Ed., Charles University: Prague, **1993**, 267.
31. Komadel, P. *Clay Minerals*. **2003**, *38*, 127.
32. Benharrats, N.; Belbachir, M.; Legran, A. P and D'espinose de le Caillerie, J. B. *Clays Minerals*. **2003**, *38*, 49.
33. Samajovà, E.; Kraus, I and Lajcàkovà, A. *Geol. Carpath. Ser. Clay*s. **1992**, *4*2, 21.
34. Tkàc, I.; Komadel P and Müle, D. *Clay Mine*r. **1994**, *2*9, 11.
35. Njopwouo, D.; Roques, G and Wandji, R. *Clay Miner.* **1987**, *22*, 45.
36. Kadokawa, J.; Iwasaki, Y and Tagaya, H. *Green Chemistry*. **2002**, *4*, 14.
37. Crivello, J. V and Fan, M. *J. Polym. Sci*. Part A. **1992**, *30*, 1.
38. Oguni, N.; Maeda, S and Tani, H. *Macromolecules*. **1973**, *6*, 459.
39. Ishimori, M.; Tsukigawa, T and Tsuruta, T. *Makromol.Chem*. **1976**, *177*, 1221.